THE JOURNAL OF PHYSICAL CHEMISTRY C

Article

pubs.acs.org/JPCC

First Principles Design of Dye Molecules with Ullazine Donor for Dye Sensitized Solar Cells

Jie Feng,[†,§] Yang Jiao,[†,§] Wei Ma,[†] Md. K. Nazeeruddin,[‡] Michael Grätzel,[‡] and Sheng Meng*[,†]

[†]Beijing National Laboratory for Condensed Matter Physics and Institute of Physics, Chinese Academy of Sciences, 100190 Beijing, China

[‡]Laboratory of Photonics and Interfaces, Swiss Federal Institute of Technology (EPFL), CH-1015 Lausanne, Switzerland

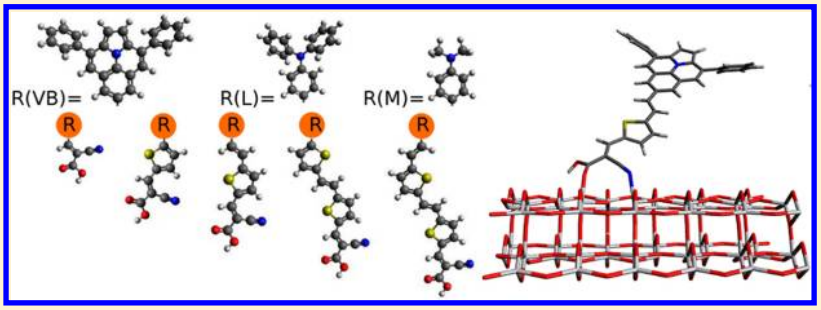

ABSTRACT: We design a series of metal-free donor-π-bridge molecules (denoted VB0−VB4) based on a new donor group—ullazine donor—as sensitizers for dye sensitized solar cell (DSSC) applications. Density functional theory (DFT) and time-dependent DFT calculations reveal that the physical properties of dyes, including spectral response, light harvesting efficiency, and electron injection rate, are systematically improved by combining ullazine donor to a series of length changing π bridges. Dye VB2 is the best candidate thanks to its outstanding performance on key parameters and achieving a balance between competing factors. Compared to two other series of molecules—L and M dyes, which differ from VB dyes by only the donor group—VB dyes have the largest light harvesting efficiency and the largest number of electrons injected to the conduction band of TiO_2. These results suggest that the ullazine group can serve as an excellent donor for future DSSC applications.

INTRODUCTION

Since the enlightening paper published in *Nature* by O'Regan and Grätzel in 1991,[1] dye-sensitized solar cells (DSSCs) have drawn comprehensive attention as one of the most promising renewable energy devices. Typical DSSCs are composed of dye molecules anchored on nanocrystalline TiO_2 deposited on transparent conducting oxide glass, platinized counter electrode, and redox electrolyte. The highest energy conversion efficiency of 12.3% under AM 1.5 irradiation has been achieved.[2] DSSCs based on conventional Ru-based chromophores such as N3/N719[3] and the black dyes[4] have been investigated intensively. However, heavy metal ions employed in metal-based dyes are scarce in nature and not environmentally friendly. Meanwhile, the synthesis and purification processes of these dyes are complicated, which prevent them from large-scale fabrication. Fortunately, metal-free organic dyes provide a prospective alternative to Ru-based dyes for their benign environmental effects, high molecular extinction coefficients, and cheap preparation processes.[5] These advantages meet the technical requirements toward utilizing a thinner TiO_2 layer to reduce energy loss during electron transport, making metal-free organic dyes ideal candidates in DSSC devices.

Most metal-free organic dyes adopt a donor-π-acceptor (D-π-A) structure, with the acceptor (A) ligand anchored on the semiconductor surface. This structure will favor efficient charge transfer of excited electrons to the conduction band of semiconductor and the regeneration of excited dyes to the ground state by the redox shuttle. Arylamine and 2-cyanoacrylic acid are the typical donor and acceptor groups employed, respectively.[6] To reach high energy conversion efficiency, the dyes must meet a series of severe requirements.[7] There should be a large driving force to ensure efficient electron injection, and the dyes' ground state oxidation potential should be higher than that of the redox couple in electrolyte to guarantee fast regeneration of the oxidized dyes. The dye acceptor, also acting as the anchor to semiconductor substrate, should be strongly adsorbed to provide stable charge transfer channels and fast electron injection. Finally, the bridge group is carefully selected to maximize sunlight absorption by shifting the spectrum from UV light to visible and near-infrared light[8] and to facilitate charge separation upon photoexcitation.

Chemical modification on individual dye units is an effective way to tune the redox potential and absorption properties of D-π-A organic dyes.[5,9,10] For instance, by changing different π spacers and electron acceptors, a red-shift in absorption spectra and significant differences in the redox potential are achieved for triphenylamine dyes.[10] Theoretical methods based on

Received: October 23, 2012
Revised: February 2, 2013
Published: February 7, 2013

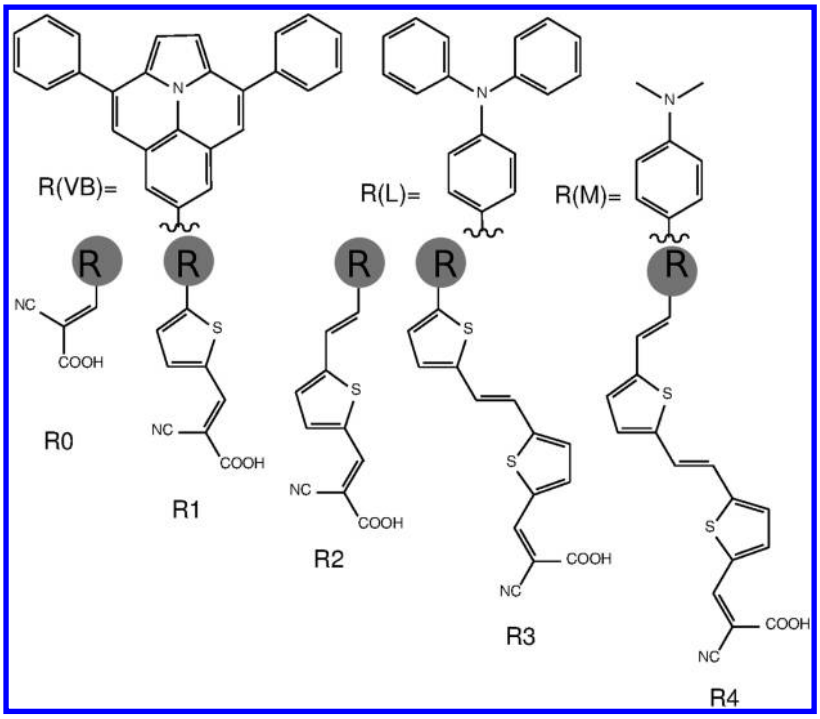

Figure 1. The donor units, R, of the three series of dyes (VB, L, M) are shown in the upper row. With R replaced by R(VB) in the lower row we could get VB0, VB1, ..., VB4 dyes.

density functional theory (DFT) and time-dependent DFT (TDDFT) calculations were also employed to rationally optimize optical and electrochemical properties of dye molecules.[8,11−13] Examples include identifying dye structures by optimizing the π spacer[8] and the acceptor group of dyes.[11] However, despite all these extensive works, there were few studies on the effects of systematic modifications of the donor group. The geometry, electrophilicity, and polarizability will directly influence the dye adsorption, spectra response, and electrodynamics. In this work we will investigate the influence of different donor groups on the performance of DSSCs by systematically evaluating the key DSSC factors determining solar cell efficiency. Rational design of dye structures based on first-principles can significantly facilitate test and development of new dyes, reducing the cost and time consumed in conventional trial-and-error experimental approaches.[14,15]

By taking advantages of theoretical approaches, we investigate an electron-rich molecular unit, ullazine donor, which has been recently synthesized experimentally[16] (structure shown in Figure 1), to be used as part of dye sensitizers for DSSC application. The nitrogen-containing heterocycle of ullazine group (Figure 1, top left) with 16 π-electrons will facilitate a strong intramolecular charge transfer. It could serve as both an electron donor and an acceptor under different conditions, which indicates a good potential for future optoelectronic applications.[16] The ullazine group has a large planar structure which will benefit patterning on the surfaces. The structure is relatively simple that could be easily manipulated in experiments and modeled in first principles calculations. The resultant dyes with ullazine donor, denoted as VB series of dyes, show near-red optical absorption and high extinction coefficients. We expect this group of dyes with ullazine donor act as high efficient candidates for DSSCs.

To systematically tune the dye's photoabsorption and electrochemical properties, we choose 2-cyanoacrylic acid as electron acceptor and anchoring group and alkene/thiophene fragments as the π spacer. By inserting alkene and thiophene between the donor and the acceptor groups, we can gradually change the energy levels of the highest occupied molecule orbital (HOMO) and the lowest unoccupied molecular orbital (LUMO) of the sensitizer and extend major absorption peak from the UV-light region to near-infrared. This results in a series of dye molecules VB0, VB1, ..., VB4, with distinct optical and electrochemical characters (Figure 1). The dye's structure and performance are optimized in terms of achieving a balance among competing factors such as light harvesting, spectral response, electronic driving force, and open circuit voltage for DSSC applications. For comparison, we take L dyes with a diphenylaminophenyl donor (R(L) in Figure 1), which were intensively studied in the literature,[17] and M dyes with a dimethylaminophenyl donor (R(M) in Figure 1), as control groups. Both L dyes and M dyes own the same π spacer and acceptor as VB dyes——they only differ by the donor group. We found that VB dyes have higher extinction coefficients, and the number of electrons injected into the semiconductor conduction band is almost 2 times larger for VB dyes than for L or M dyes, resulting from stronger electronic interactions between VB molecules and the TiO_2 surface.

METHODS

The sunlight-to-electricity conversion efficiency (η) of solar cell devices is determined by the open-circuit photovoltage (V_{OC}), short-circuit current density (J_{SC}), and the fill factor (FF), as compared to incident solar power (P_{inc}):

$$\eta = \mathrm{FF}\frac{V_{OC}J_{SC}}{P_{inc}} \quad (1)$$

In DSSCs, we can calculate the V_{OC} as[17]

dx.doi.org/10.1021/jp310504n | J. Phys. Chem. C 2013, 117, 3772−3778

$$V_{OC} = \frac{E_C + \Delta CB}{q} + \frac{kT}{q}\ln\left(\frac{n_c}{N_{CB}}\right) - \frac{E_{redox}}{q} \quad (2)$$

Here q is the unit charge, E_c is the conduction band edge (CBE) of the semiconductor substrate, k is the Boltzmann constant, T is the absolute temperature, n_c is the number of electrons in the conduction band, N_{CB} is the density of accessible states in the conduction band,[8] and E_{redox} is the reduction−oxidation potential of electrolyte. ΔCB is the shift of E_c when the dyes are adsorbed on substrate and can be expressed as[18]

$$\Delta CB = \frac{q\mu_{normal}\gamma}{\varepsilon_0\varepsilon} \quad (3)$$

In this expression, μ_{normal} denotes the dipole moment of individual dye molecules perpendicular to the surface of the semiconductor substrate and γ is the dyes' surface concentration. ε_0 and ε represent the vacuum permittivity and the dielectric permittivity, respectively. It is obvious from eqs 2 and 3 that n_c and μ_{normal} exert crucial influences on V_{OC}.

The J_{SC} in DSSCs is determined by the following equation:[8]

$$J_{SC} = \int LHE(\lambda)\Phi_{inject}\eta_{collect}\, d\lambda \quad (4)$$

where LHE(λ) is the light harvesting efficiency at a given wavelength, Φ_{inject} evinces the electron injection efficiency, and $\eta_{collect}$ denotes the charge collection efficiency. In the systems which are only different in sensitizers, $\eta_{collect}$ can be reasonably assumed to be constant. LHE(λ) can be calculated with

$$LHE = 1 - 10^{-f} \quad (5)$$

where f represents the oscillator strength of adsorbed dye molecules. Φ_{inject} is related to the driving force ΔG_{inject} of electrons injecting from the excited states of dye molecules to the semiconductor substrate. It can be estimated as[19]

$$\Delta G_{inject} = E^{dye*} - E_{CB} = E^{dye} + E_{0-0} - E_{CB} \quad (6)$$

where E^{dye*} is the oxidation potential of the excited dye, E^{dye} is the redox potential of the ground state of the dye, E_{0-0} is the vertical transition energy, and E_{CB} is the conduction band edge of the semiconductor. So J_{SC} can be well estimated through f and ΔG_{inject}.

On the basis of eqs 1−6, we could roughly predict the efficiency of novel dyes without intensive calculations. More insightful theoretical estimations could be achieved using DFT-based real-time evolution of electron dynamics as in our previous works.[20,21] However, the calculations are rather expensive (with thousands of CPU hours per trajectory). We believe the present approach will be interesting and valuable for assisting experimentalists in searching for high performance dyes. All the calculations are performed based on DFT and TDDFT.[22] Ground-state geometry optimization is carried out with SIESTA code. During the optimization, we use Troullier−Martins pseudopotentials[23] to represent the atomic cores, generalized gradient approximation (GGA) as exchange-correlation functional,[24] a double-ξ plus polarization basis sets of localized orbitals with an energy cutoff of 100 Ry, and the optimization will stop when the force on each atom is smaller than 0.02 eV/Å in magnitude. We also use the Gaussian09 program package to simulate the absorption spectra of all dyes in vacuum with CAM-B3LYP exchange-correlation functional and the energy levels of the dyes' molecule orbitals with B3LYP exchange-correlation functional. The 6-31G(d) basis sets were used for C, H, O, N, and S. This set of parameters is illustrated to produce nice agreements with experiment.[11]

RESULTS

Structure and Properties of VB Dyes. The optimized structure of VB series of dyes is shown in Figure 1. Dye VB0 is composed by ullazine donor directly connected to the cyanoacrylic acid acceptor group. Dye VB1 has an additional thiophene group inserted as a linker. The linker group in dye VB2 is further elongated by adding an alkene group. Dyes VB3 and VB4 were formed by extending the π spacer by another thiophene group or by a thiophene and a new alkene group, respectively. This series of VB dyes, from VB0 to VB4, are gradually elongated by extending the π spacer.

To demonstrate their characteristic electronic structure, we choose three representative VB dyes—VB0, VB2, and VB4—and plot the distribution of molecular orbital wave functions in Figure 2. Wave functions of VB1 and VB3 dyes have similar

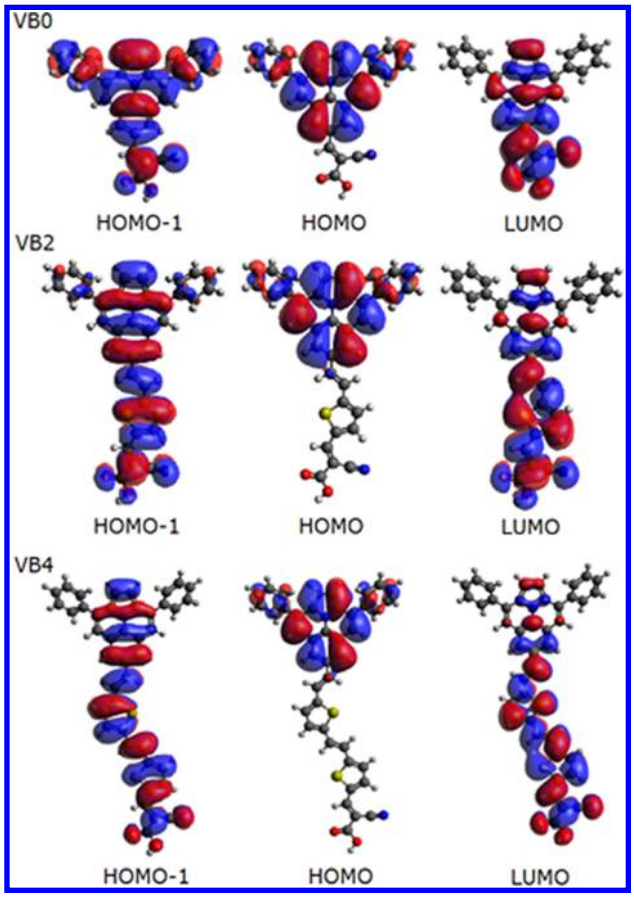

Figure 2. Frontier molecular orbitals of VB0, VB2, and VB4 dyes. A typical D-π-A character is shown.

features. As expected, the distribution of molecular orbitals of VB dyes show a strong D-π-A character; namely, the HOMO orbitals are localized on the donor part while the LUMO orbitals are mainly localized on the cyanoacrylic acceptor group of the molecule. The HOMO-1 orbitals of all dyes are more or less delocalized over the entire molecule. The π-characters of these orbitals will contribute to high extinction coefficients of the VB series of dyes. The D-π-A charge distribution favors a strong electron−hole separation on TiO_2 surface, which is

dx.doi.org/10.1021/jp310504n | J. Phys. Chem. C 2013, 117, 3772−3778

preferred for efficient electron injection from the electronically excited dye to the semiconductor.

Chemical modifications in the linker group would tune photoabsorption of VB dyes, since it is well-known that longer π linkers favor red-shifted absorption in D-π-A dyes. We then calculate the UV−vis absorption spectrum of VB dyes, shown in Figure 3, to analyze one of the key factors in DSSC, LHE.

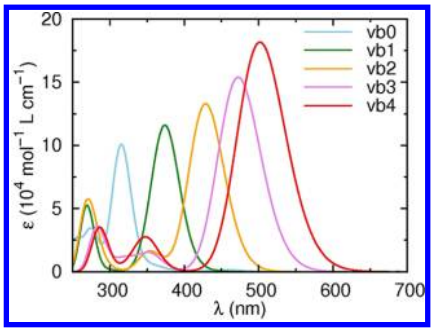

Figure 3. Calculated absorption spectra of VB dyes.

The extinction coefficient is evaluated following the procedures in ref 11. Table 1 shows that the wavelength for maximum absorption, λ_{max}, is shifted from ultraviolet range (315.3 nm for VB0) to blue-green range (501.8 nm for VB4) as the linker gets longer. The red-shifted absorption spectrum matches better solar spectrum, which has a maximal intensity at ∼500 nm. Higher efficiencies could be achieved with dyes showing more red-shifted light absorbance. Experiments also reveal that dyes (JD21) with the acceptor group linked to the side position of ullazine (site 5 instead of site 6) yield additional merits with maximum absorption at 582 nm and light conversion efficiency of 8%.[16] Our calculations reproduce the absorption spectrum nicely. In this work, we will focus on the effect of substituting the donor with novel ullazine groups. Results on systematic modifications of ullazine dyes with acceptors at different positions will be presented elsewhere. The oscillator strength of all the five dyes is large and increases with the length of the π spacer, and so does the LHE. The calculated LHEs are all near unity. The longest dye VB4 has the largest oscillator strength and LHE. TDDFT with traditional exchange-correlation functionals tends to underestimate the excitation energy especially for charge transfer transitions of molecules. The errors increase with the decrease in overlap between the orbitals of the ground and excited states. Hybrid functional will reduce the errors, and with long-range corrections the errors are further decreased to a level of ∼0.5 eV, making the discrepancy between experiment and theory less dependent on the coupling degrees of initial and final states in optical transitions.[25] It should be noticed that in VB dyes the main contribution to the first absorption peak is assigned to a charge transfer (CT) transition from HOMO-1 to LUMO, which is different from most D-π-A organic dye molecules, where electron excitation from HOMO to LUMO plays a critical role. This is caused by the symmetry of the molecular orbitals: strong separation between the HOMO and LUMO levels in VB dyes makes their spatial overlap very small, resulting in a negligible oscillator strength <0.03 for HOMO → LUMO electronic transitions.

We note that ullazine dyes have been successfully synthesized in experiment recently[16] after we have carried out theoretical characterizations of VB dyes. An ullazine dye, JD32, which only slightly differ from the VB1 dye (phenylhexyloxy group in JD32 versus phenyl group in VB1 on the peripheral of ullazine donor) was reported[16] with a major absorption peak at 393 nm and a small shoulder at 540 nm. For comparison, we predicted that the dye have maximum adsorption at 376 nm (oscillator strength = 1.49) and a very small shoulder at ∼500 nm (oscillator strength = 0.01, small shoulders are not listed in Table 1), in consistence with experiment. The small difference is attributed to structural difference in the donor as well as computational errors in DFT exchange-correlation functionals. Solar cells fabricated with JD32 (VB1) dyes present acceptable light-to-electricity efficiency of 2%. Higher efficiencies will be achieved with dyes with more red-shifted light absorbance. Experiments also reveal that dyes (JD21) with the acceptor group linked to the side position of ullazine (site 5 instead of site 6) yield additional merits with maximum absorption at 582 nm and light conversion efficiency of 8%. Our calculations reproduce the absorption spectrum of these dyes nicely. Results on systematic modifications of this group of ullazine dyes with acceptors at the different position will be presented elsewhere.

Figure 4 shows the calculated energy levels of the VB dyes. As the linker getting longer the HOMO-1 are upshifted for almost 1 eV and the LUMO downshift for about 0.5 eV. This is in agreement with the increase in the λ_{max}. On the other hand,

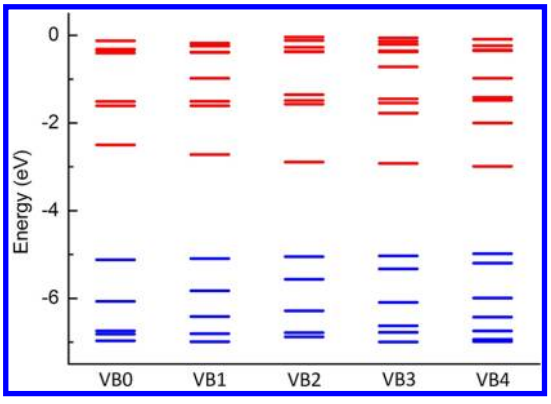

Figure 4. Calculated energy levels of molecular orbitals of VB dyes. The red bars denote unoccupied orbitals, and blue ones denote occupied orbitals.

Table 1. Calculated Maximum Absorption Wavelength (λ_{max}), Oscillator Strengths (f), Light Harvesting Efficiency (LHE), and the Corresponding Electronic Transitions for VB Dyes

dye	λ_{max} (nm)	f	LHE (λ)	assignment
VB0	315.3	1.39	0.959	H-1 → L(67%) H → L+1(16%) H-2 → L(9%)
VB1	375.8	1.49	0.968	H-1 → L(69%) H-2 → L(13%) H → L+2(9%)
VB2	428.6	1.83	0.985	H-1 → L(88%) H-2 → L(7%)
VB3	472.6	2.12	0.992	H-1 → L(87%)
VB4	501.8	2.51	0.997	H-1 → L(85%)

dx.doi.org/10.1021/jp310504n | J. Phys. Chem. C 2013, 117, 3772−3778

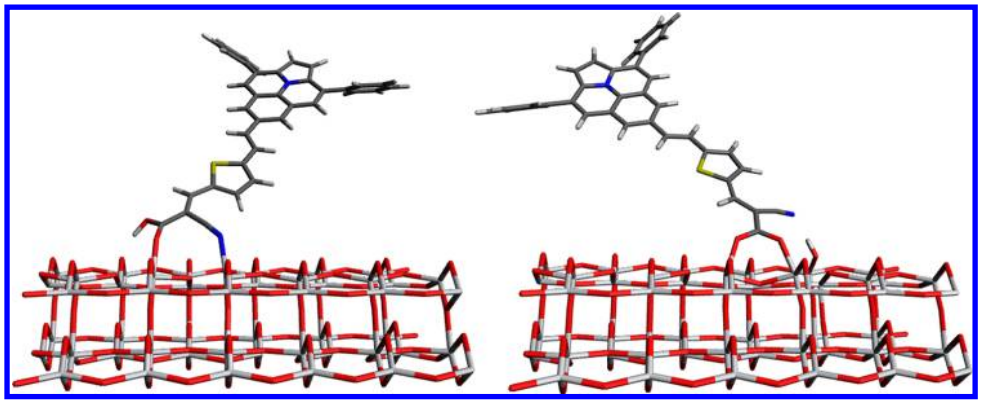

Figure 5. Two adsorption configurations of dyes on TiO_2 (101) surface: N^O adsorption (left) and O^O adsorption (right).

the HOMO level does not shift much. This could be understood since the HOMO is strongly localized on the donor part and does not change its characteristics as the π spacer elongates. Some may argue that after photoexcitation from the HOMO-1 to LUMO level the presence of higher lying HOMO may deteriorate DSSC performance. We note that the energy level of HOMO orbitals, about −5.0 eV, is sufficiently lower than the redox potential of I^-/I_3^- electrolyte at −4.6 eV.[26] In addition, this character could provide an advantage to separately optimize the optical absorption and the regeneration potential of dye sensitizers. Ru-based high efficiency dyes, for instance C101 and C106 with efficiency larger than 11%, have similar HOMO levels (−5.34 and −5.05 eV, respectively). Long-term stability under moderate thermal stress and visible-light soaking has been proved in experiments.[27] Some metal-free dyes also show a HOMO level in the range of −5.1 to −5.2 eV and present high efficiencies up to 9%.[28]

Dye Adsorption onto TiO_2 Surfaces. On the basis of the knowledge of isolated dyes, we extend to study the energy alignment, electronic coupling, and interface dipole moment of these dyes when adsorbed onto TiO_2 substrate to analyze other factors affecting the energy conversion efficiency. TiO_2 anatase (101) surface is modeled using a slab with a thickness of six atomic layers. Periodic boundary conditions are employed, with a surface supercell of 10.24 × 22.70 $Å^2$ and a vacuum layer of at least 10 Å to prevent the interactions between adjacent slabs. Two adsorption configurations are considered (see Figure 5). The N^O adsorption configuration has the C−N and one of the two C−O groups in cyanoacrylic carboxylic acid binding to the surface Ti atoms. The H in carboxylic acid forms a hydrogen bond with the surface O atom. The O^O configuration denotes the configuration that both O atoms in the carboxylic acid group form a Ti−O bond with surface Ti atoms. In the latter adsorption mode, the dye is deprotonated to have H from the carboxylic acid covalently bound to a surface O atom during geometry relaxation. The N^O adsorption is more stable for all dyes considered here (see adsorption energies listed in Table 2), consistent with our previous findings. This configuration is then adopted for further discussion. Representative VB0, VB2, and VB4 dyes are taken as examples, since other dyes show qualitatively the same trend.

Following eq 6, we calculated driving force ΔG_{inject}, listed in Table 3, to estimate the injection efficiency Φ_{inject}. From VB0, VB2, to VB4, the reduction potential of the conduction band E_{CB} increases as the dipole moment μ_{normal} pointing out of the surface gets larger. At the same time, the $E^{dye}*$ decreases so ΔG_{inject} and thus Φ_{inject} decrease (see Figure 6). Considering that the LHE increases with the length of the linker group, we need to find a balance between competing Φ_{inject} and LHE to reach a large J_{SC}.

Table 2. Computed Adsorption Energies (in eV)

adsorption	VB0	VB2	VB4	L2	M2
N^O	1.39	1.28	1.25	1.30	1.33
O^O	0.84	0.87	0.91	0.90	0.93

Table 3. Calculated Electronic Properties of VB0, VB2, and VB4 Adsorbed onto TiO_2 Anatase (101)

dye	E^{dye} (eV)	E_{0-0} (eV)	$E^{dye}*$(eV)	E_{CB} (eV)	ΔG_{inject} (eV)	μ_{normal} (D)	n_c
VB0	−6.38	3.93	−2.45	−4.17	1.72	8.67	0.72
VB2	−6.03	2.89	−3.14	−4.05	0.91	11.66	0.12
VB4	−5.71	2.47	−3.24	−3.95	0.71	16.38	0.04

We could also estimate the V_{OC} through eq 2. It is reasonable to assume N_{CB} and E_{redox} to be constant for different dyes as they are determined by the properties of the substrate and electrolyte, respectively. The conduction band edge of semiconductor could be extracted from projected density of states calculations (E_{CB} in Table 3). The temperature of 300 K and typical N_{CB} density of 7×10^{20} cm^{-3} are adopted.[8] The dye loading density[6] is on the scale of 100 mmol cm^{-3}. Then $kT \ln(n_c/N_{CB})$ is calculated to be 0.11, 0.06, and 0.03 eV for VB0, VB2, and VB4, respectively. However, the effect of electron occupation in conduction band is relatively small compared to the influence of surface dipole moment. As a result, the V_{OC} for VB2 and VB4 are 0.07 and 0.14 V larger, respectively, than VB0. In real devices, dark current is another influencing factor that must be considered. Experiments show that longer dye may cause larger dark current.[6] Possible reasons include the loss of surface protection for long dye and flexible donor groups binding to the surface. Taking all above considerations, we expect that VB2 will show a proper V_{OC} in devices. Other factors affecting energy conversion efficiency including dye loading concentration, dye aggregation, and desorption are out of the scope of this paper and will be investigated in future work.

Comparison to Dyes with a Different Donor. Compared to L and M series of dyes, VB dyes have an obviously larger donor group. In general, a large donor unit

dx.doi.org/10.1021/jp310504n | J. Phys. Chem. C 2013, 117, 3772−3778

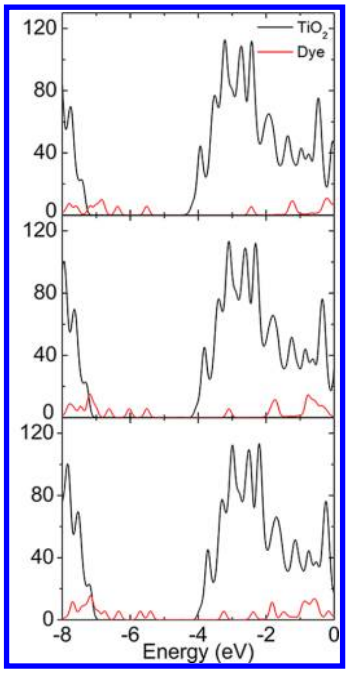

Figure 6. Projected density of states (PDOS) of VB0, VB2, and VB4 adsorbed on TiO_2 anatase (101) surface. The unoccupied states of the dye have been upshifted according to the vertical excitation energy from TDDFT calculations.

could prevent electrolyte from contact with the semiconductor substrate, effectively blocking charge recombination between TiO_2 and the electrolyte and reducing the unfavorable aggregation of dyes at the semiconductor surface.[29] Therefore, VB dyes would be more favorable in DSSC applications over L and M series of dyes. To make a more accurate evaluation of VB dye characteristics and the potential utilizations in DSSCs, we compare the distinct properties among VB2, L2, and M2 dyes, which are different only in the donor unit (see Figure 1).

As shown in Table 4, although VB2 has maximum absorption at λ_{max} = 429 nm, slightly smaller than M2 (452 nm) and L2 (462 nm), VB2 presents the largest oscillator strength, leading to the largest LHE in turn. When VB2 adsorbed on TiO_2 semiconductor substrate, the ΔG_{inject} is slightly smaller than that of L2 and M2. However, an energy difference of 0.91 eV between dye LUMO and TiO_2 CBE is large enough to guarantee efficient electron injection. On the other hand, too large ΔG_{inject} may introduce energy redundancy, resulting a smaller V_{OC} and large thermalization losses.[29] In the latter process the interactions between excited charge carrier and lattice phonons would have the carrier cooled down to the bandgap edge, losing its initial high potential energy. More importantly, the number of transferred electrons in TiO_2 conduction band upon VB2 adsorption is almost twice that for L2 and M2. This implies a stronger surface polarization and electronic coupling between VB2 and the TiO_2 substrate. Also, a large electron transfer will favor a higher V_{OC}. As the conduction band edge of TiO_2 E_{CB} is located at −4.05 and −4.18 V respectively upon VB2 and L2 adsorption, the V_{OC} will be 0.13 V larger for VB2 dye than for L2. The enhanced LHE and higher V_{OC} suggest that VB2 is more suitable for highly efficient DSSCs.

CONCLUSION

In conclusion, we report a new type of donor group, ullazine donor, to be used for organic dye sensitized solar cells. By lengthening the π bridge, we successfully increase the dye's light harvesting efficiency and dipole moment, and we find VB2 is the best among all the five VB dyes because it performs nicely on the four key parameters (λ_{max}, LHE, ΔG_{inject}, V_{OC}) and achieves a good balance among these factors. Furthermore, compared with widely adopted existing donor groups, diphenylaminophenyl and dimethylaminophenyl donors, application of the new ullazine donor shows an enhanced extinction coefficient and LHE, an increased number of electrons transferred to conduction bands of TiO_2, and a high V_{OC}. In addition, the photoabsorption property and regeneration potential of VB dyes could be separately optimized. All these characteristics suggest VB dyes a competitive candidate for all-organic, highly efficient, near-red absorption DSSCs.

AUTHOR INFORMATION

Corresponding Author

*E-mail: smeng@iphy.ac.cn.

Author Contributions

The manuscript was written through contributions of all authors. All authors have given approval to the final version of the manuscript.

Author Contributions

§These authors contributed equally.

Notes

The authors declare no competing financial interest.

ACKNOWLEDGMENTS

This work is partly supported by NSFC (grant 11074287) and MOST (grant 2012CB921403) and hundred talent program of CAS.

REFERENCES

(1) O'Regan, B.; Grätzel, M. A Low-Cost, High-Efficiency Solar Cell Based on Dye-Sensitized Colloidal TiO_2 Films. *Nature* **1991**, *353* (6346), 737−740.

(2) Yella, A.; Lee, H.-W.; Tsao, H. N.; Yi, C.; Chandiran, A. K.; Nazeeruddin, M. K.; Diau, E. W.-G.; Yeh, C.-Y.; Zakeeruddin, S. M.; Grätzel, M. Porphyrin-Sensitized Solar Cells with Cobalt (II/III)-

Table 4. Calculated Optical and Electronic Nature of VB2, L2, and M2 Dyes[a]

dye	λ_{max} (nm)	f	LHE	assignment	ΔG_{inject} (eV)	μ_{normal} (D)	n_c
VB2	428.6	1.83	0.985	H-1 → L(88%) H-2 → L(7%)	0.91	11.66	0.12
L2	462.3	1.71	0.980	H → L(83%) H-1 → L(11%)	1.01	14.30	0.07
M2	452.2	1.51	0.969	H → L(91%)	0.98	16.86	0.06

[a]The three groups are only different in their donor groups.

Based Redox Electrolyte Exceed 12% Efficiency. *Science* **2011**, *334* (6056), 629−634.
(3) (a) Nazeeruddin, M. K.; Kay, A.; Rodicio, I.; Humphry-Baker, R.; Mueller, E.; Liska, P.; Vlachopoulos, N.; Grätzel, M. Conversion of Light to Electricity by cis-X_2Bis(2,2′-bipyridyl-4,4′-dicarboxylate)-ruthenium(II) Charge-Transfer Sensitizers (X = Cl^-, Br^-, I^-, CN^-, and SCN^-) on Nanocrystalline Titanium Dioxide Electrodes. *J. Am. Chem. Soc.* **1993**, *115* (14), 6382−6390. (b) Nazeeruddin, M. K.; Zakeeruddin, S. M.; Humphry-Baker, R.; Jirousek, M.; Liska, P.; Vlachopoulos, N.; Shklover, V.; Fischer, C.-H.; Grätzel, M. Acid−Base Equilibria of (2,2′-Bipyridyl-4,4′-dicarboxylic acid)ruthenium(II) Complexes and the Effect of Protonation on Charge-Transfer Sensitization of Nanocrystalline Titania. *Inorg. Chem.* **1999**, *38* (26), 6298−6305.
(4) Péchy, P.; Renouard, T.; Zakeeruddin, S. M.; Humphry-Baker, R.; Comte, P.; Liska, P.; Cevey, L.; Costa, E.; Shklover, V.; Spiccia, L.; Deacon, G. B.; Bignozzi, C. A.; Grätzel, M. Engineering of Efficient Panchromatic Sensitizers for Nanocrystalline TiO_2-Based Solar Cells. *J. Am. Chem. Soc.* **2001**, *123* (8), 1613−1624.
(5) Hagfeldt, A.; Boschloo, G.; Sun, L.; Kloo, L.; Pettersson, H. Dye-Sensitized Solar Cells. *Chem. Rev.* **2010**, *110* (11), 6595−6663.
(6) Hagberg, D. P.; Marinado, T.; Karlsson, K. M.; Nonomura, K.; Qin, P.; Boschloo, G.; Brinck, T.; Hagfeldt, A.; Sun, L. Tuning the HOMO and LUMO Energy Levels of Organic Chromophores for Dye Sensitized Solar Cells. *J. Org. Chem.* **2007**, *72* (25), 9550−9556.
(7) Kim, S.; Lee, J. K.; Kang, S. O.; Ko, J.; Yum, J. H.; Fantacci, S.; De Angelis, F.; Di Censo, D.; Nazeeruddin, M. K.; Grätzel, M. Molecular Engineering of Organic Sensitizers for Solar Cell Applications. *J. Am. Chem. Soc.* **2006**, *128* (51), 16701−16707.
(8) Zhang, J.; Li, H.-B.; Sun, S.-L.; Geng, Y.; Wu, Y.; Su, Z.-M. Density Functional Theory Characterization and Design of High-Performance Diarylamine-fluorene Dyes with Different π Spacers for Dye-Sensitized Solar Cells. *J. Mater. Chem.* **2012**, *22* (2), 568−576.
(9) Cai, N.; Moon, S.-J.; Cevey-Ha, L.; Moehl, T.; Humphry-Baker, R.; Wang, P.; Zakeeruddin, S. M.; Grätzel, M. An Organic D-π-A Dye for Record Efficiency Solid-State Sensitized Heterojunction Solar Cells. *Nano Lett.* **2011**, *11*, 1452−1456.
(10) Tian, H.; Yang, X.; Chen, R.; Zhang, R.; Hagfeldt, A.; Sun, L. Effect of Different Dye Baths and Dye-Structures on the Performance of Dye-Sensitized Solar Cells Based on Triphenylamine Dyes. *J. Phys. Chem. C* **2008**, *112*, 11023−11033.
(11) Meng, S.; Kaxiras, E.; Nazeeruddin, M. K.; Grätzel, M. Design of Dye Acceptors for Photovoltaics from First-Principles Calculations. *J. Phys. Chem. C* **2011**, *115* (18), 9276−9282.
(12) Casanova, D.; Rotzinger, F. P.; Grätzel, M. Computational Study of Promising Organic Dyes for High-Performance Sensitized Solar Cells. *J. Chem. Theory Comput.* **2010**, *6*, 1219−1227.
(13) Pastore, M.; Mosconi, E.; De Angelis, F.; Grätzel, M. A Computational Investigation of Organic Dyes for Dye-Sensitized Solar Cells: Benchmark, Strategies, and Open Issues. *J. Phys. Chem. C* **2010**, *114*, 7205−7212.
(14) Hachmann, J.; Olivares-Amaya, R.; Atahan-Evrenk, S.; Amador-Bedolla, C.; Sánchez-Carrera, R. S.; Gold-Parker, A.; Vogt, L.; Brockway, A. M.; Aspuru-Guzik, A. The Harvard Clean Energy Project: Large-Scale Computational Screening and Design of Organic Photovoltaics on the World Community Grid. *J. Phys. Chem. Lett.* **2011**, *2*, 2241−2251.
(15) Li, R.; Lv, X.; Shi, D.; Zhou, D.; Cheng, Y.; Zhang, G.; Wang, P. Dye-Sensitized Solar Cells Based on Organic Sensitizers with Different Conjugated Linkers: Furan, Bifuran Thiophene, Bithiophene, Selenophene, and Biselenophene. *J. Phys. Chem. C* **2009**, *113*, 7469−7479.
(16) Delcamp, J. H.; Yella, A.; Holcombe, T. W.; Nazeeruddin, M. K.; Grätzel, M. The Molecular Engineering of Organic Sensitizers for Solar-Cell Applications. *Angew. Chem., Int. Ed.* **2012**, DOI: 10.1002/anie.201205007.
(17) Marinado, T.; Nonomura, K.; Nissfolk, J.; Karlsson, M. K.; Hagberg, D. P.; Sun, L.; Mori, S.; Hagfeldt, A. How the Nature of Triphenylamine-Polyene Dyes in Dye-Sensitized Solar Cells Affects the Open-Circuit Voltage and Electron Lifetimes. *Langmuir* **2009**, *26* (4), 2592−2598.
(18) Rühle, S.; Greenshtein, M.; Chen, S. G.; Merson, A.; Pizem, H.; Sukenik, C. S.; Cahen, D.; Zaban, A. Molecular Adjustment of the Electronic Properties of Nanoporous Electrodes in Dye-Sensitized Solar Cells. *J. Phys. Chem. B* **2005**, *109* (40), 18907−18913.
(19) Katoh, R.; Furube, A.; Yoshihara, T.; Hara, K.; Fujihashi, G.; Takano, S.; Murata, S.; Arakawa, H.; Tachiya, M. Efficiencies of Electron Injection from Excited N3 Dye into Nanocrystalline Semiconductor (ZrO_2, TiO_2, ZnO, Nb_2O_5, SnO_2, In_2O_3) Films. *J. Phys. Chem. B* **2004**, *108* (15), 4818−4822.
(20) Meng, S.; Kaxiras, E. Electron and Hole Dynamics in Dye-Sensitized Solar Cells: Influencing Factors and Systematic Trends. *Nano Lett.* **2010**, *10*, 1238−1247.
(21) Jiao, Y.; Zhang, F.; Grätzel, M.; Meng, S. Structure-Property Relations in All-Organic Dye-Sensitized Solar Cells. *Adv. Funct. Mater.* **2013**, *23*, 424−429.
(22) (a) Kohn, W.; Sham, L. J. Self-Consistent Equations Including Exchange and Correlation Effects. *Phys. Rev.* **1965**, *140* (4A), A1133−A1138. (b) Runge, E.; Gross, E. K. U. Density-Functional Theory for Time-Dependent Systems. *Phys. Rev. Lett.* **1984**, *52* (12), 997−1000.
(23) Troullier, N.; Martins, J. L. Efficient Pseudopotentials for Plane-Wave Calculations. *Phys. Rev. B* **1991**, *43* (3), 1993−2006.
(24) Perdew, J. P.; Burke, K.; Ernzerhof, M. Generalized Gradient Approximation Made Simple. *Phys. Rev. Lett.* **1996**, *77* (18), 3865−3868.
(25) Manzhos, S.; Segawa, H.; Yamashita, K. Computational Dye Design by Changing the Conjugation Order: Failure of LR-TDDFT to Predict Relative Excitation Energies in Organic Dyes Differing by the Positions of the Methine Unit. *Chem. Phys. Lett.* **2012**, *527*, 51−56.
(26) Zhang, G.; Bala, H.; Cheng, Y.; Shi, D.; Lv, X.; Yu, Q.; Wang, P. High Efficiency and Stable Dye-Sensitized Solar Cells with an Organic Chromophore Featuring a Binary π-Conjugated Spacer. *Chem. Commun.* **2009**, 2198−2200.
(27) (a) Gao, F.; Wang, Y.; Zhang, J.; Shi, D.; Wang, M.; Humphry-Baker, R.; Wang, P.; Zakeeruddin, S. M.; Grätzel, M. A New Heteroleptic Ruthenium Sensitizer Enhances the Absorptivity of Mesoporous Titania Film for a High Efficiency Dye-Sensitized Solar Cell. *Chem. Commun.* **2008**, 2635−2637. (b) Cao, Y.; Bai, Y.; Yu, Q.; Cheng, Y.; Liu, S.; Shi, D.; Gao, F.; Wang, P. Dye-Sensitized Solar Cells with a High Absorptivity Ruthenium Sensitizer Featuring a 2-(Hexylthio)thiophene Conjugated Bipyridine. *J. Phys. Chem. C* **2009**, *113*, 6290−6297.
(28) (a) Hwang, S.; Lee, J. H.; Park, C.; Lee, H.; Kim, C.; Park, C.; Lee, M.-H.; Lee, W.; Park, J.; Kim, K.; Park, N.-G.; Kim, C. A Highly Efficiency Organic Sensitizer for Dye-Sensitized Solar Cells. *Chem. Commun.* **2007**, 4887−4889.
(29) (a) Ning, Z.; Zhang, Q.; Wu, W.; Pei, H.; Liu, B.; Tian, H. Starburst Triarylamine Based Dyes for Efficient Dye-Sensitized Solar Cells. *J. Org. Chem.* **2008**, *73* (10), 3791−3797. (b) Sayama, K.; Tsukagoshi, S.; Hara, K.; Ohga, Y.; Shinpou, A.; Abe, Y.; Suga, S.; Arakawa, H. Photoelectrochemical Properties of J Aggregates of Benzothiazole Merocyanine Dyes on a Nanostructured TiO_2 Film. *J. Phys. Chem. B* **2002**, *106* (6), 1363−1371.